International Journal of Mechanical, Industrial and Aerospace Sciences
ISSN: 2517-9950
Vol:5, No:6, 2011

Slug tracking simulation of severe slugging experiments

Tor Kindsbekken Kjeldby, Ruud Henkes and Ole Jørgen Nydal

Abstract—Experimental data from an atmospheric air/water terrain slugging case has been made available by the Shell Amsterdam research center, and has been subject to numerical simulation and comparison with a one-dimensional two-phase slug tracking simulator under development at the Norwegian University of Science and Technology. The code is based on tracking of liquid slugs in pipelines by use of a Lagrangian grid formulation implemented in C++ by use of object oriented techniques. An existing hybrid spatial discretization scheme is tested, in which the stratified regions are modelled by the two-fluid model. The slug regions are treated incompressible, thus requiring a single momentum balance over the whole slug.

Upon comparison with the experimental data, the period of the simulated severe slugging cycle is observed to be sensitive to slug generation in the horizontal parts of the system. Two different slug initiation methods have been tested with the slug tracking code, and grid dependency has been investigated.

Keywords—hydrodynamic initiation, slug tracking, terrain slugging, two-fluid model, two-phase flow

I. Introduction

Slug flow is a dynamic flow regime which plays an important role in a wide range of industrial multiphase pipe flow applications. Major attention to dynamic two-phase flow modelling was initiated by the introduction of nuclear power generation and its reliance on two-phase steam-water flow. Another industrial field in which slug flow represents an important challenge is in the oil and gas industry, where liquids and gas may be transported over long distances in form of multiphase mixtures. In such systems, the slugs may potentially become long and hence represent operational challenges as they periodically enter receiving facilities, giving sudden increases in liquid loading on separators and other equipment.

The modelling of slug flow may be approached in different ways. A common procedure is to solve the two-fluid equations on an Eulerian grid. This is a procedure typically used by nuclear safety codes like CATHARE and RELAP [1], [2], as well as tailored oil and gas simulators like OLGA [3]. In the recent years a series of contributions have been given to investigate the capabilities of the two-fluid model on calculating flow regime transitions directly, without the need for any supplementary transition criteria [4], [5]. These computational contributions are classified as slug capturing simulations, and rely on the application of a fine grid in order to resolve all details within the flow. Alternatively a unit-cell approach in which slug flow is treated in an averaged manner within each section may be utilized. This allows for larger cell lengths and is the procedure used in OLGA.

Another option is to apply a Lagrangian grid formulation. This allows for direct tracking of fronts and elimination of numerical diffusion at discontinuities. This is the concept utilized by the slug tracking code SLUGGIT. The concept and initial code formulation was originally developed by [6] and was implemented in C++ by use of object oriented techniques. This allows for large flexibility with respect to code re-use and ease of modification in selected regions of the computational domain. Several follow-up contributions have been given to the concept of moving grid slug tracking and the investigation of different discretization and solving procedures [7], [8],[9],[10].

The simulations presented in this paper have been made with a model based on the code version developed by [10]. The objective is to simulate a series of terrain slugging experiments made available by the Shell Amsterdam research center, in which the generation of hydrodynamic slugs in horizontal parts of the system can influence the overall dynamics and slug frequency. The code is based on a formulation in which the complete two-fluid model is solved in the stratified Taylor bubble regions, and an overall momentum balance is performed over incompressible slugs.

II. The model

The spatial discretization of the governing conservation equations is implemented in terms of a hybrid two-fluid model formulation. In stratified sections the full two-fluid model is implemented, while in slug sections a simplified approach is followed. This allows for the application of a single momentum balance over each slug unit, as slugs are treated as incompressible. This may potentially contribute to increase simulation efficiency in systems where long slugs are present. The organization of computational objects into units, sections and borders is illustrated in Figure 1.

The mass balance for phase k is given by Equation (1) in which ρ_k denotes density of phase k, V_k volume of phase k, u_k phase velocity and A_k cross-section area of phase k. The term $\dot{M}_k^s$ is a mass source of phase k. The boundary grid velocity is denoted u_b. Mass balances are performed for all sections.

$$\frac{\partial(\rho_k V_k)}{\partial t} + \int_{A_k} \rho_k (u_k - u_b) dS = \dot{M}_k^s \tag{1}$$

Expanding the term $\frac{\partial(\rho_k V_k)}{\partial t}$ in Equation (1) by use of the product rule and adding together Equation (1) for all phases allows for the derivation of the pressure equation, Equation (2). Here, p denotes pressure.

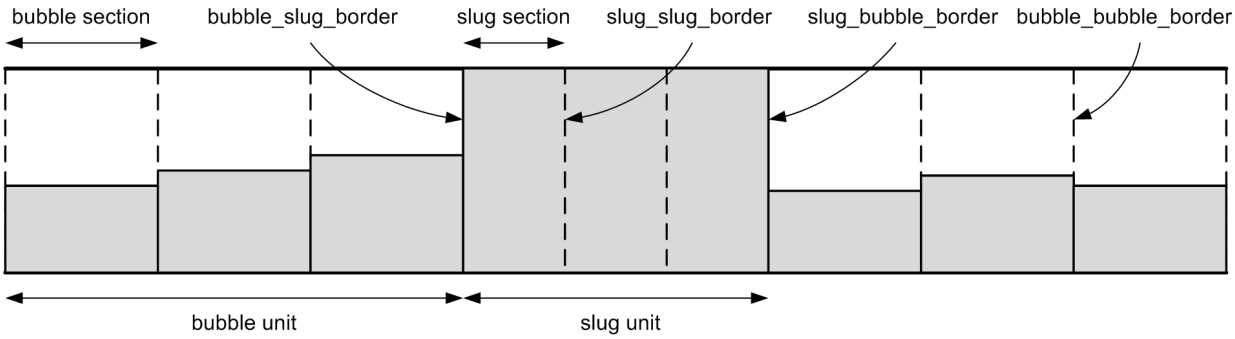

Fig. 1: Data structure with units, sections and borders

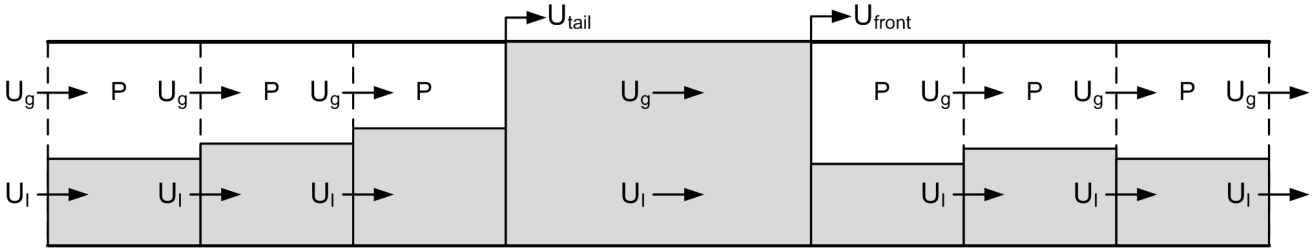

Fig. 2: Grid

$$\sum_k \frac{V_k}{\rho_k}\left(\frac{\partial \rho_k}{\partial p}\right)_T \frac{\partial p}{\partial t} + \frac{\partial V}{\partial t} + \sum_k \frac{1}{\rho_k}\int_{A_k} \rho_k (u_k - u_b) dS = \sum_k \frac{\dot{M}_k^s}{\rho_k} \tag{2}$$

The derivative of density with respect to pressure for phase k, $\frac{\partial \rho_k}{\partial p}$, is obtained from a general equation of state Equation (3) or by interpolation in a PVT table during each time step. The pressure equation is solved for all bubble sections as shown in Figure 2.

$$\rho_k = \rho_k(p, T) \tag{3}$$

The momentum equation for phase k is given by Equation (4). The shear stress τ_{kw} between phase k and the pipe wall is determined from Equation (5) and the wall friction factor λ_{kw}, which is determined from the Haaland correlation given by Equation (6). The pipe inclination is given by θ and the height of the liquid film is given by h_l. The gravitational acceleration is denoted g.

The arrows shown in Figure 2 represent phase velocities and illustrate that the momentum equations are solved at bubble-bubble borders and in slug units. A staggered pressure-velocity scheme is hence used. The single momentum balance applied for each slug unit in combination with zero gas fraction in slugs implies that the phase velocities are the same within all sections in a slug unit.

$$\begin{aligned} &\tfrac{\partial(\rho_k V_k u_k)}{\partial t} + \int_{A_k} \rho_k (u_k - u_b) u_k dS = \\ &-V_k \tfrac{\partial p}{\partial x} - \rho_k V_k g \cos\theta \cdot \tfrac{\partial h_l}{\partial x} + \int_{A_k} \tau_k dS - \rho_k V_k g \sin\theta \end{aligned} \tag{4}$$

$$\tau_{kw} = \frac{1}{8}\lambda_{kw}\rho_k |u_k| u_k \tag{5}$$

$$\frac{1}{\sqrt{\lambda_{kw}}} = -1.8 \cdot \log\left[\frac{6.9}{\mathrm{Re}_k} + \left(\frac{\varepsilon}{3.7 D_{h,k}}\right)^{1.11}\right] \tag{6}$$

The interface friction is determined as a multiplum of the gas-wall friction and an interfacial friction multiplier denoted IFM from Equation (7). $IFM = 1.0$ has been used for the simulations in this paper. The hydraulic diameters of gas and liquid are given by Equation (8) and (9) respectively.

$$\tau_i = \frac{1}{8} \cdot IFM \cdot \lambda_{gw}\rho_g |u_g - u_l| (u_g - u_l) \tag{7}$$

$$D_{h,g} = \frac{\pi D^2}{S_g + S_i} \tag{8}$$

$$D_{h,l} = \frac{\pi D^2}{S_l} \tag{9}$$

An important closure parameter for this model is the bubble nose velocity U_b. This velocity may typically be expressed by a relation on the form given in Equation (10). Several experimental investigations have been given to establish empirical correlations for the coefficients C_0 and U_0, where [11] and [12] were some of the earlier.

$$U_{tail} = U_b = C_0 U_m + U_0 \tag{10}$$

The correlations used for the slug tracking code are given by [13], with a correction for slug length dependency given by [14].

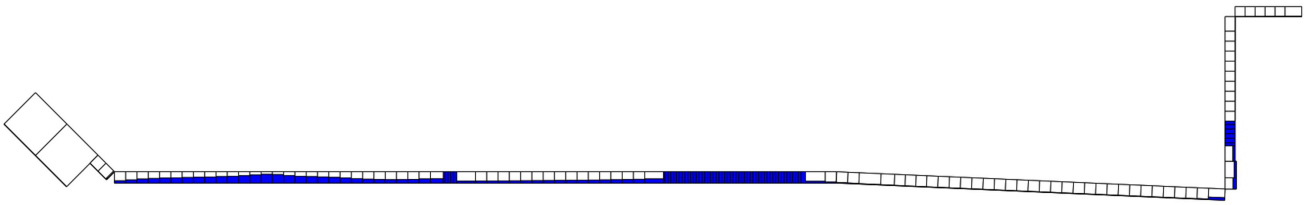

Fig. 3: Simulation geometry

The slug front velocity U_{front} is determined from a mass balance across the slug front given by Equation (11). For the code to determine whether a bubble-slug discontinuity is a slug front or a bubble nose, a bubble turning criterion is needed. The criterion used in the current code version is simply that bubble noses always travel towards low pressure.

$$U_{front} = \frac{U_l - H_{bubble}U_{l,bubble}}{1 - H_{bubble}} \tag{11}$$

Initiation of hydrodynamic slugs is made according to flow regime criteria. The viscous Kelvin Helmholtz criterion (VKH) has been applied for the current simulations. When the transition criterion is satisfied in a bubble section, a slug is initiated. This procedure represents a numerical perturbation in flow variables which affects the nearby region, and a certain number of time steps have to be executed without the transition criterion enabled in order to bring the systems back to stable behaviour.

A delay constant C_{delay} is used to provide this required delay in seconds before the transition criterion is made active again. This delay is given by Equation (12).

$$\Delta t_{delay} = C_{delay} \cdot \frac{D}{|U_l|} \tag{12}$$

The solution algorithm for the slug tracking code can be summarized by the following steps:

1) Solve pressure and momentum equations, Equation (2) and (4), simultaneously by Gaussian Elimination of banded matrix
2) Solve mass equations, Equation (1), by Gaussian Elimination of banded matrix
3) Update equation of state, Equation (3)
4) Section management operations with splitting and merging of computational sections and initiation or removal of slugs

III. The simulation geometry

The simulated terrain slugging experiments originate from the Shell Amsterdam research center. Figure 3 shows a screenshot of the dynamic animation tool called PLOTIT which is used to animate results from SLUGGIT. The shown simulation geometry has been chosen to as close as possible reproduce the experimental geometry. The large diameter pipe in the leftmost part of the window has been included to simulate a 250 [L] air buffer tank at the inlet. This tank was included in the experiments to provide upstream compressibility which is vital for the severe slugging cycle to occur. It should be noted that the shown diameters have been scaled to make it easier to examine the liquid holdup profile represented by blue color. For a correct impression of the length to diameter ratios, consult Table I.

The inlet boundary has been implemented in terms of a closed boundary with zero phase velocities. Gas is introduced by a gas source in the buffer tank. The outlet border is open with a fixed pressure equal to the atmospheric. The liquid source is included in PIPE 3.

TABLE I: Simulation geometry

Pipe	Length [m]	Diameter [m]	Roughness [m]	Inclination θ [°]
1	7.958	0.2000	1E-5	-45.00
2	2.000	0.0508	1E-5	-45.00
3	0.100	0.0508	1E-5	-45.00
4	65.000	0.0508	1E-5	0.00
5	35.000	0.0508	1E-5	-2.54
6	2.500	0.0508	1E-5	90.00
7	13.000	0.0450	1E-5	90.00
8	4.000	0.0450	1E-5	0.00
9	2.000	0.0450	1E-5	0.00

IV. Slug initiation from the two-fluid model

The period of the terrain slugging cycle is observed to be dependent on the liquid accumulation in the horizontal PIPE 4 and the generation of hydrodynamic slugs shown in Figure 4. When a hydrodynamic slug is formed it represents a complete blockage to the gas flow. It is hence accelerated in downstream direction and absorbs the liquid in the stratified layer ahead of it. The location of initiation does hence influence how much liquid is removed from the horizontal pipe during each cycle.

A series of SLUGGIT simulations were performed without any kind of explicit slug initiation model to check if slugs could be initiated from the two-fluid model itself. The results are shown in Figure 5 in terms of slugging cycle period plotted against grid spacing Δx. The period obtained for simulations performed with the VKH as initiation model are also plotted in Figure 5 and correspond to the simulations presented at the second line from the bottom in Table II.

Even though the maximum grid spacing applied is 40D, hydrodynamic slug generation directly from the two-fluid model itself is observed. The simulated period is observed to approach the experimental period as the grid spacing is reduced. One reason for this can be that a fine grid gives contributions to move the point of slug initiation towards the inlet of the horizontal pipe. One should expect the simulated period to approach the experimental period as grid spacing is further decreased in analogy with the concept of slug capturing. It has however not been possible to obtain stable simulations for

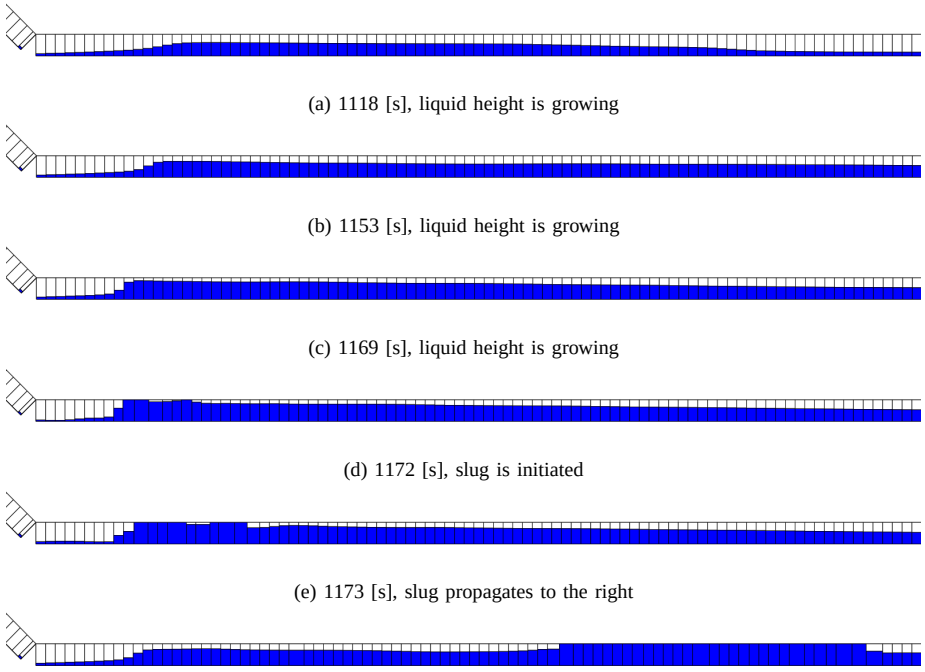

(a) 1118 [s], liquid height is growing

(b) 1153 [s], liquid height is growing

(c) 1169 [s], liquid height is growing

(d) 1172 [s], slug is initiated

(e) 1173 [s], slug propagates to the right

(f) 1185 [s], slug propagates to the right

Fig. 4: Slug generation

grid spacing smaller than 5D. This has probably to do with ill-posedness problems as the amount of numerical diffusion is reduced.

Some of the simulations which were performed with the finest grid and which were difficult to make run stable as mentioned above were observed to become more robust and possible to run for long times when the option of slug initiation from the VKH criterion was enabled.

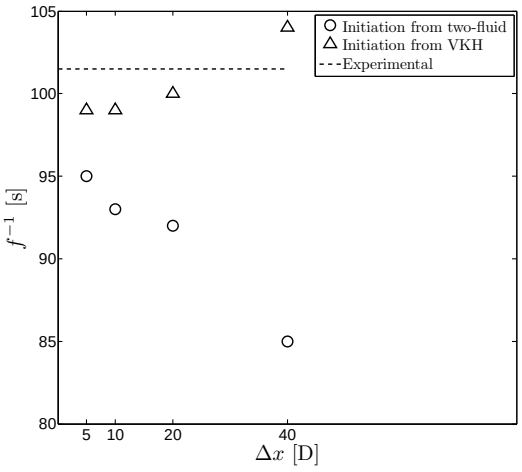

Fig. 5: Severe slugging frequency with changing grid size

The period of the slugging cycle is also observed to be sensitive to the inlet configuration and the location of the water source. Figure 6 shows a picture of the experimental inlet configuration. Air is supplied to the horizontal pipe from the buffer tank by the large diameter pipe. Liquid is supplied by the small diameter pipe which is connected to the downward inclined part of the larger diameter pipe.

Simulations were first made by inclusion of the liquid source in the first computational cell inside the horizontal pipe, as the momentum contribution from the injected water was assumed to be negligible. This neglection of momentum source was however observed to give liquid accumulation and rapid slug initiation. A different approach was hence chosen to avoid this problem. The liquid source was instead connected to a short PIPE 3 upstream the horizontal PIPE 4. This allowed for gravitational influence on the water which in turn caused the water to enter PIPE 4 with a limited velocity, hence reducing the liquid accumulation and immediate slug initiation. The minimum slug length where slugs disappear is 1D for all simulations in this paper.

V. Grid dependency

As demonstrated in Section IV, the initiation of slugs from the two-fluid model itself without any explicit slug initiation criterion is highly dependent on the grid spacing Δx. For further simulations the VKH has therefore been used as initiation criterion for the SLUGGIT simulations. The choice of the delay parameter C_{delay} can also influence on the results. Sensitivity on grid spacing and the C_{delay} has been tested for the combination of flow rates defined as Case 1 in Table III. The results are shown in Table II. Based on this sensitivity analysis, a grid spacing of 20D in combination with $C_{delay} = 20$ has been used for the simulations presented in Section VI.

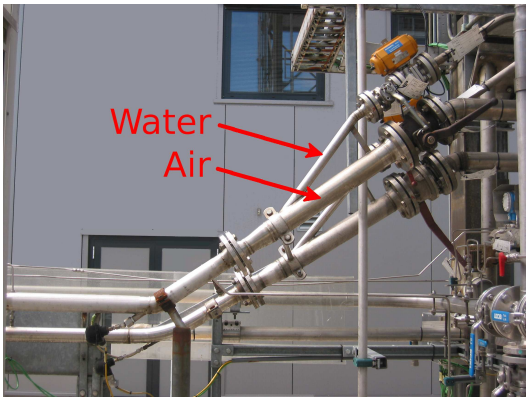

Fig. 6: Experimental inlet configuration

TABLE II: Sensitivity on Δx and C_{delay} measured in terms of slugging cycle period $\bar{f}$ [s]

	Δx [D]			
C_{delay}	**5**	**10**	**20**	**40**
5	99	101	100	101
10	100	101	99	103
20	99	99	100	104
40	99	98	99	102

VI. Simulation of three experimental cases

Experimental time series for three different combinations of superficial air and water velocities have been chosen for plotting together with time series from slug tracking simulations. The three combinations of superficial velocities are given in Table III. The time series represent pressure at the inlet of the riser (PIPE 6) in [Pa].

TABLE III: Experimental cases

Case	$U_{sl}[m/s]$	$U_{sg}[m/s]$
1	0.20	1.80
2	0.11	0.90
3	0.40	3.60

Comparison of the time series for Case 1 and Case 2 reveals relatively close correspondence between experiment and simulation. The simulated period is observed to be some lower than the experimental period in Case 1 and some higher in Case 2. Some deviation can also be observed upon comparison of the maximum pressure values. The simulated maximum pressure values are observed to be some lower than the experimental.

Once during each cycle the pressure is observed to drop quickly. This is due to the mechanism where liquid starts propagating up the vertical pipe. The drop in pressure is however observed to be more gradual in the experiments, compared to what is observed in the simulations.

The slightly too low maximum pressures and the too steep drop in pressure may possibly relate to how slugs are generated at the low-point between PIPE 5 and PIPE 6. One would expect liquid to flow towards this low-point from both PIPE 5 and PIPE 6 during certain parts of the severe slugging cycle, both due to liquid fall-back from PIPE 6 and due to liquid supply from the upstream part of the system. This liquid will give an increase in liquid holdup in the bend, and result in the generation of a short slug at the moment when the liquid bridges the whole cross-section. No specific section management operations are performed to handle this mechanism in the current code version. Consequently, slug generation in the bend relies on the general slug initiation criterion, which implies that no slugs will be created before the holdup in the bend exceeds 0.99. The length of the slugs generated at the low-point will hence depend on the length of the neighbouring bubble sections and the time needed to fill them with liquid. A more frequent generation of shorter slugs would probably have contributed to a more gradual simulated drop in pressure and possibly a higher maximum pressure.

A section management routine tailored to handle slug generation at low-points has earlier been tested with success in the code version by [6], and will in the future be implemented in the current code version.

The process where liquid accelerates up the vertical pipe gives an increase in gas velocity in the horizontal pipe and subsequent generation of a hydrodynamic slug as illustrated in Figure 4. This slug gives rise to the relatively quick buildup in pressure which is observed to follow shortly after each distinct drop in pressure in Figure 7a and 7b.

Comparison between experiments and simulations in Case 3 reveals less good correspondence between simulation and experiment. The gas and liquid flow rates are higher, and inspection of the experimental time series indicates that stable flow conditions have been reached with some signs left of cyclic behaviour, possibly indicating that the Case 3 characteristics are in the vicinity of transition to terrain slugging II. The unstable behavior observed in the simulated Case 3 is, similarily to the deviations in Case 1 and Case 2, likely to originate from how slugs are handled at the low-point.

VII. Conclusion

Relatively good correspondence between experiments and simulations has been observed in the two experimental cases where distinct severe slugging behavior is observed. In the third case where more stable flow conditions are observed in the experiments, less good correspondence between experiment and simulation is observed. The simulation gives a pressure time series showing a more unstable behavior than what was observed in the experiments. This is likely to result from how slug generation at low-points is handled in the current code. A section management routine specifically developed to take care of this mechanism will hence be implemented in the coming.

With respect to slug generation in horizontal pipes, satisfactory results have been obtained with the viscous Kelvin Helmholtz criterion. Slug generation directly from the two-fluid model has also been tested. This method does however rely on the application of a fine grid, which is typially applied in slug capturing codes and is hence probably less suited for

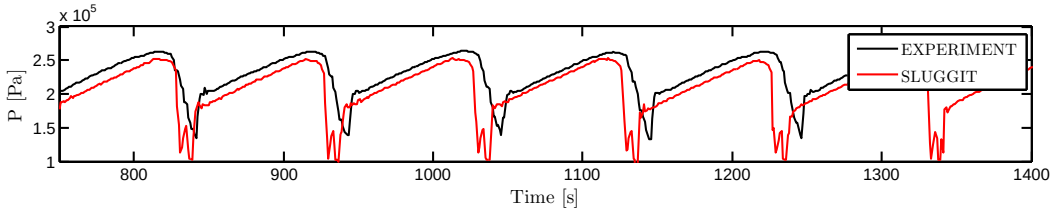

(a) Case 1

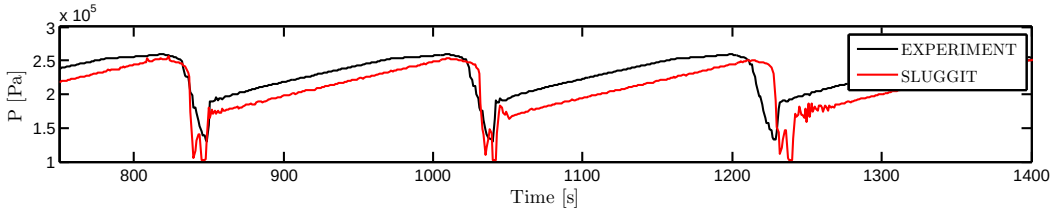

(b) Case 2

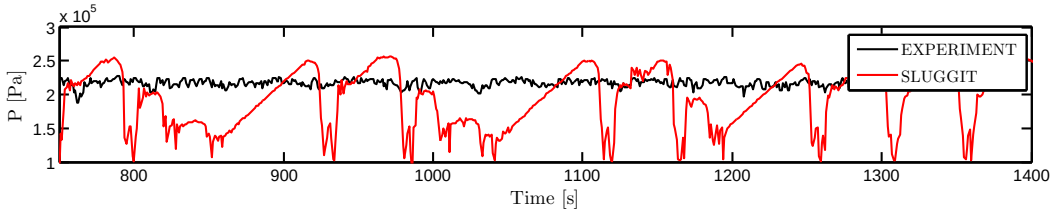

(c) Case 3

Fig. 7: Simulation of 3 experimental cases

the Lagrangian grid slug tracking concept where larger grid spacing is generally used.

Acknowledgement

Tor Kindsbekken Kjeldby acknowledges Jon Egdetveit Seim (Shell, Stavanger) who conducted the Case 1, 2 and 3 experiments during work with his master thesis in Shell, and Ruud Henkes (Shell Amsterdam) who has made the experimental data available. Ondra Novak (NTNU) has currently implemented a series of changes and improvements in the PLOTIT code which has proven very useful during testing of the SLUGGIT code.

References

[1] D. Bestion, The physical closure laws in the cathare code, Nuclear Engineering and Design 124 (1990) 229–245.
[2] RELAP5/MOD3.3 CODE MANUAL VOLUME IV: MODELS AND CORRELATIONS.
[3] K. Bendiksen, D. Malnes, R. Moe, S. Nuland, The dynamic two-fluid model olga: Theory and application, SPE Production Engineering (1991) 171–180.
[4] R. Issa, M. Kempf, Simulation of slug flow in horizontal and nearly horizontal pipes with the two-fluid model, International Journal of Multiphase Flow 29 (2003) 69–95. doi:10.1016/S0301-9322(02)00127-1.
[5] M. Bonizzi, P. Andreussi, S. Banerjee, Flow regime independent, high resolution multi-field modelling of near-horizontal gas-liquid flows in pipelines, International Journal of Multiphase Flow 35 (1) (2009) 34 – 46. doi:DOI: 10.1016/j.ijmultiphaseflow.2008.09.001.
[6] O. Nydal, S. Banerjee, Dynamic slug tracking simulations for gas-liquid flow in pipelines, Chem. Eng. Comm. 141-142 (1996) 13–39.
[7] A. D. Leebeeck, A roll wave and slug tracking scheme for gas-liquid pipe flow, Ph.D. thesis, NTNU (2010).
[8] F. Renault, A lagrangian slug capturing scheme for gas-liquid flows in pipes, Ph.D. thesis, NTNU (2007).
[9] P. Klebert, Slug tracking, PostDoc work (2004).
[10] J. Kjølås, Plug propagation in multiphase pipelines: Modeling and small scale experiments, Ph.D. thesis, NTNU (2007).
[11] D. T. Dumitrescu, Strömung an einer luftblase im senkrechten rohr, Z. angew. Math. Mech 23 (3) (1943) 139–149.
[12] R. M. Davies, G. Taylor, The mechanics of large bubbles rising through extended liquids and through liquids in tubes, The Royal Society, series A, Mathematical and Physical sciences 200 (1062) (1950) 375–390.
[13] K. Bendiksen, An experimental investigation of the motion of long bubbles in inclined tubes, International Journal of Multiphase Flow 10 (4) (1984) 467 – 483. doi:DOI: 10.1016/0301-9322(84)90057-0.
[14] R. Moissis, P. Griffith, Entrance effects in a two-phase slug flow, Journal of Heat Transfer 84 (1962) 366–370.

Tor Kindsbekken Kjeldby is a PhD candidate at Department of Energy and Process Engineering at the Norwegian University of Science and Technology, Trondheim. (e-mail: tor.kjeldby@ntnu.no)

Ruud Henkes is a Principal Technical Expert on Fluid Flow at the Shell Research Centre, Amsterdam and a part-time Professor of Multiphase pipeline flows at Delft University of Technology. (e-mail: ruud.henkes@shell.com)

Ole Jørgen Nydal is a Professor at Department of Energy and Process Engineering at the Norwegian University of Science and Technology, Trondheim. (e-mail: ole.j.nydal@ntnu.no)